

Coordinate-Independent Robot Model Identification

Yanhao Yang, Ross L. Hatton

Abstract—Robot model identification is commonly performed by least-squares regression on inverse dynamics, but existing formulations measure residuals directly in coordinate force space and therefore depend on the chosen coordinate chart, units, and scaling. This paper proposes a coordinate-independent identification method that weights inverse-dynamics residuals by the dual metric induced by the system Riemannian metric. Using the force-velocity vector-covector duality, the dual metric provides a physically meaningful normalization of generalized forces, pulling coordinate residuals back into the ambient mechanical space and eliminating coordinate-induced bias. The resulting objective remains convex through an affine-metric and Schur-complement reformulation, and is compatible with physical-consistency constraints and geometric regularization. Experiments on an inertia-dominated Crazyflie-pendulum system and a drag-dominated LandSalp robot show improved identification accuracy, especially on shape coordinates, in both low-data and high-data settings.

I. INTRODUCTION

Accurate robot dynamic models are central to modern robotics. They underpin model-based control [1], simulation for robot learning [2], state estimation [3], trajectory optimization [4], and hardware design [5], especially in regimes where performance, safety, and sample efficiency matter. Whether the goal is dexterous manipulation, agile locomotion, marine propulsion, or interaction with uncertain environments, model quality strongly affects downstream performance [6]. In practice, however, first-principles models are rarely exact: unmodeled friction, fluid effects, compliance, manufacturing tolerances, and parameter uncertainty all create a gap between nominal and real behavior [7]. Robot model identification therefore remains a fundamental problem, providing a systematic way to estimate dynamic parameters from data and reduce this modeling gap [8].

A broad range of identification methods has been developed in robotics. Classical approaches include frequency-response identification [9], least-squares fitting of inverse dynamics [10], and residual fitting on nominal models [11]. More recent data-driven methods incorporate geometric mechanics [12], dynamic mode decomposition [13], self-supervised learning [14], neural differential models [15], and physics-informed learning [16].

Among these methods, inverse-dynamics least squares remains one of the most widely used tools in practice because it leverages physical priors, often reduces identification to a linear or convex regression problem, scales well to large

This work was supported in part by NSF Grants No. 1653220, 1826446, and 1935324, and by ONR Grant No. N00014-23-1-2171.

Y. Yang and R. L. Hatton are with the Collaborative Robotics and Intelligent Systems (CoRIS) Institute at Oregon State University, Corvallis, OR USA. {yangyanh, Ross.Hatton}@oregonstate.edu

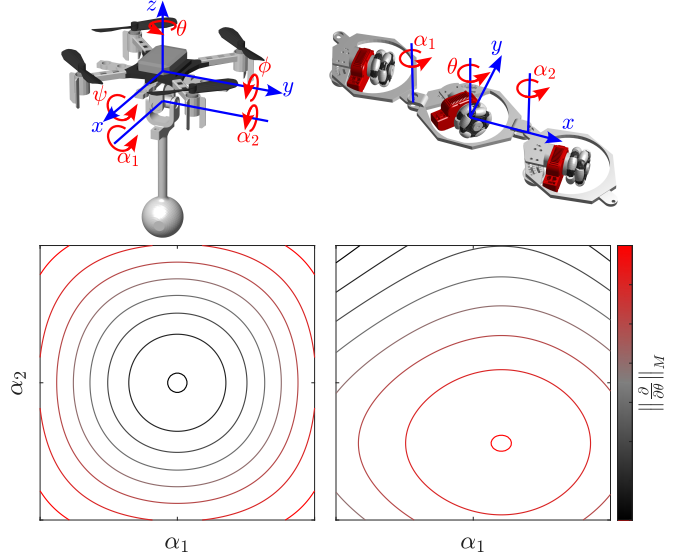


Fig. 1. Two robotic systems studied in this paper for model identification: an inertia-dominated system (left) and a drag-dominated system (right). In both systems, the generalized coordinates have different units and scales, and the magnitude of the inner product of a unit coordinate velocity under the corresponding Riemannian metric depends on the configuration, as illustrated in the bottom-left and bottom-right panels, which plot the inner-product value along the θ direction for the two systems, respectively. Together, these factors illustrate the coordinate dependence in the system identification problem addressed in this paper.

datasets, avoids repeated forward simulation, and integrates naturally with constraints and priors [8]. It is a general approach for estimating rigid-body inertial parameters, and analogous formulations also arise in systems dominated by other generalized linear constitutive effects [17].

The key limitation of inverse-dynamics least squares, however, is geometric rather than computational. Its standard formulation is typically derived from a maximum-likelihood viewpoint under isotropic Gaussian residual assumptions, which leads to minimizing a Euclidean norm of residuals in coordinate generalized force space. This assumption implicitly treats all coordinates as commensurate and measures error according to the chosen coordinate chart rather than the underlying mechanics. Consequently, the identified model can depend on the units, scaling, or parameterization of the generalized coordinates. Coordinates expressed in radians, meters, or rescaled internal variables may contribute very differently to the objective even when they represent physically comparable effects. This issue is especially pronounced in systems with heterogeneous coordinates, multiple scales, or configuration-dependent metric distortion, such as the two systems in Fig. 1. In such cases, Euclidean residual

minimization can bias the fit toward coordinates with numerically larger force magnitudes, leading to models that fit one coordinate representation well but generalize poorly across equivalent reparameterizations.

Several extensions improve inverse-dynamics least squares, but they do not fully resolve this coordinate dependence. Weighted least squares based on error covariance accounts for measurement uncertainty [18]; regularization improves conditioning and reduces overfitting in data-limited settings [18]; physically consistent constraints enforce realizable inertial parameters [19]; and energy-based residuals attempt to better reflect physical structure [20]. These methods improve robustness, stability, and physical plausibility, but their weightings are typically introduced for statistical, numerical, or prior-based reasons rather than from the intrinsic dual structure of mechanics. As a result, the residual objective usually remains coordinate dependent. Energy-based objectives partially avoid direct force-residual minimization, but they also compress the information in the full inverse-dynamics equations and can reduce identifiability. Thus, a principled treatment of coordinate independence in inverse-dynamics identification is still lacking.

This paper addresses that gap by introducing a dual-metric-weighted least-squares formulation for inverse dynamics. For robot systems whose dynamics are governed by a Riemannian metric on the configuration manifold, generalized velocities are tangent vectors and generalized forces are cotangent vectors (“covectors”) in the cotangent space dual to the tangent space. The natural metric on force space is therefore not the implicit Euclidean metric used in standard least squares, but the dual metric induced by the Riemannian metric on velocities. Weighting inverse-dynamics residuals by this dual metric yields a physically meaningful normalization rooted in the force–velocity vector–covector duality through power. In effect, this pulls coordinate force residuals back into the ambient mechanical space, eliminating dependence on arbitrary coordinate scaling and reparameterization while preserving the computational advantages of inverse-dynamics least squares. The resulting problem can still be formulated as a convex optimization problem and remains compatible with standard enhancements such as physically consistent constraints and geometric regularization.

We validate the proposed method on both inertia-dominated and drag-dominated robotic systems (Fig. 1). Across both platforms, the proposed dual-metric weighting improves identification accuracy and generalization relative to error-covariance-weighted least squares, energy-based objectives, and regularized least-squares methods with additional prior information. The advantage is most pronounced on shape coordinates, where the nonlinear coordinate representation of the configuration manifold makes coordinate dependence especially harmful, and it persists in both low-data and high-data scenarios.

II. PRELIMINARIES

This section summarizes the standard inverse-dynamics least-squares formulation for robot system identification and the main extensions relevant to this paper.

A. Inverse-Dynamics Least-Squares System Identification

We consider robot systems whose dynamics can be written in inverse-dynamics form, i.e., as a map from the measured state, state derivatives, and model parameters to applied generalized effort. Let $q \in Q$ denote generalized coordinates, \dot{q} generalized velocities, \ddot{q} generalized accelerations, $\tau \in T_q^*Q$ generalized forces (or efforts), and $\pi \in \mathbb{R}^p$ the dynamic parameter vector.

The key assumption is that the inverse dynamics is affine in the unknown parameter vector π , so it can be written as a regression in the parameters. Then, for each sample k ,

$$\tau_k = Y(q_k, \dot{q}_k, \ddot{q}_k)\pi + \varepsilon_k, \quad (1)$$

where $Y(\cdot) \in \mathbb{R}^{n \times p}$ is the regressor matrix, n is the number of generalized coordinates, and ε_k collects measurement noise, unmodeled effects, and model mismatch. The ordinary least-squares (OLS) estimate is then obtained by minimizing the squared inverse-dynamics residual:

$$\hat{\pi} = \arg \min_{\pi} \sum_{k=1}^N \|Y_k \pi - \tau_k\|_2^2. \quad (2)$$

This formulation is attractive because it avoids repeated forward simulation, preserves sample-wise separability, and reduces system identification to a convex regression problem whenever the inverse dynamics is linear in the parameters.

This affine-in-parameters structure arises in multiple physical regimes. For rigid-body systems dominated by inertia, such as the Crazyflie–pendulum system in the top left of Fig. 1, the inverse dynamics commonly takes the form

$$\tau = M(q)\ddot{q} + C(q, \dot{q})\dot{q} + g(q), \quad (3)$$

where $M(q)$ is the mass matrix, $C(q, \dot{q})\dot{q}$ collects Coriolis and centrifugal effects, and $g(q)$ is the generalized gravity term. A standard result in robot dynamics is that this model can be written linearly in a set of inertial parameters, where π may include link masses, center-of-mass moments, and inertia tensor terms.

In other robotic systems, inertial effects may be negligible relative to drag. In low-Reynolds-number locomotion, highly damped mechanisms, or systems moving through a resistive medium, such as the LandSalp robot in the top right of Fig. 1, a reduced-order model may be written as

$$\tau = M(q)\dot{q}, \quad (4)$$

where $M(q)$ is a drag or resistance matrix. If the drag model is linear in the unknown drag coefficients, then it also admits the affine form in (1), with π encoding those coefficients.

Across inertia-dominated, drag-dominated, and mixed regimes, the key requirement is not a particular physical mechanism, but rather that the inverse dynamics can be expressed as a regressor linear in the unknown parameters.

B. Improvements to Inverse-Dynamics Least Squares

Although OLS is widely used, several extensions have been proposed to improve robustness, physical plausibility, or statistical efficiency.

1) Weighted Least Squares Using Error Covariance:

If the residual ε is heteroscedastic or correlated, OLS is no longer statistically efficient. A standard generalization is weighted least squares (WLS),

$$\hat{\pi} = \arg \min_{\pi} \sum_{k=1}^N (Y_k \pi - \tau_k)^T W (Y_k \pi - \tau_k), \quad (5)$$

where typically $W = \Sigma^{-1}$ with residual covariance

$$\Sigma = \sum_{k=1}^N \mathbb{E}[\varepsilon_k \varepsilon_k^T] \succ 0. \quad (6)$$

This weighting emphasizes residual directions with lower uncertainty and downweights directions with larger noise variance [18]. In practice, W may be chosen from sensor models, empirical covariance estimates, or heuristic normalization factors. However, this weighting is still defined in the chosen coordinate chart. When that chart is nonlinear, the metric distortion can vary with configuration, so a fixed covariance-based weight does not correct the underlying coordinate dependence of the residual.

2) *Physically Consistent Constraints*: A least-squares fit may yield parameters that explain the measured data but violate physical realizability. For rigid-body identification, examples include negative mass, inertia tensors that are not positive semidefinite, or inertial parameters inconsistent with any realizable mass distribution [19]. To address this problem, identification can be formulated as a constrained optimization problem:

$$\hat{\pi} = \arg \min_{\pi} \sum_{k=1}^N \|Y_k \pi - \tau_k\|_2^2 \quad \text{s.t.} \quad P(\pi) \succ 0, \quad (7)$$

where, for mass–inertia parameters, $P(\pi)$ is the pseudo-inertia matrix, and the constraint enforces positive mass and density-realizable moments of inertia; for viscous drag coefficients, $P(\pi)$ is the drag coefficient matrix, and the constraint enforces that drag-induced dissipation is always nonpositive.

When these constraints are expressed in convex form, the resulting problem remains a convex quadratic program. Such physically consistent identification improves interpretability, extrapolation, and compatibility with downstream control and simulation.

3) *Geometric Convex Regularization*: When data are limited or the regressor is ill-conditioned, the least-squares estimate may have high variance or be vulnerable to noise or outliers. Regularization addresses this problem by penalizing undesirable parameter values or deviations from prior structure [18]. A general regularized problem is

$$\hat{\pi} = \arg \min_{\pi} \sum_{k=1}^N \|Y_k \pi - \tau_k\|_2^2 + \lambda R(\pi), \quad (8)$$

where $R(\pi)$ is a regularizer and $\lambda \geq 0$ is a tuning parameter.

Convex approximations to the geodesic distance between two positive-definite matrices can be used as regularizers. Two common examples are the Bregman divergence and the constant pullback metric evaluated at a nominal value π_0 , obtained from CAD or a previously identified model. Such geometric convex regularization can improve conditioning, reduce overfitting, and encode structured priors while preserving convexity. In practice, however, these methods depend on the availability and quality of prior information: the nominal value π_0 may be unavailable or inaccurate due to modeling simplifications, manufacturing tolerances, or wear. Moreover, the regularization strength λ must be tuned, and performance may be sensitive to that choice.

4) *Energy-Related Residuals*: Another line of work modifies the residual so that the optimization objective reflects the energetic structure of the system [20]. Instead of minimizing the coordinate force error directly, one can define residuals based on scalar energetic quantities by pairing the force residual with the measured velocity:

$$\hat{\pi} = \arg \min_{\pi} \sum_{k=1}^N (\dot{q}_k^T (Y_k \pi - \tau_k))^2. \quad (9)$$

These formulations replace the vector-valued force residual with an energy-rate residual and may better align the objective with physically meaningful scalar quantities such as work or power transfer.

However, because such residuals compress the vector-valued inverse-dynamics error into lower-dimensional energetic quantities, they may discard information contained in the full force balance. As a result, they can trade improved physical interpretability for reduced identifiability or altered statistical behavior.

III. METHODOLOGY

We now develop a coordinate-independent inverse-dynamics identification objective using the duality between generalized velocities and generalized forces. Generalized coordinates live in a chart of the configuration manifold, while the physical motion and effort they represent live in an underlying ambient mechanical space. The system Riemannian metric provides the natural way to measure velocities in that space, and the induced dual metric provides the corresponding physically meaningful way to measure force residuals. We then show that, although the resulting weighted objective depends on the unknown dynamic parameters, it can still be reformulated as a convex optimization problem.

A. Dual-Metric Weighting for Coordinate-Independent Identification

Suppose the system is equipped with a symmetric positive-definite metric tensor

$$M(q, \pi) \in \mathbb{S}_{++}^n, \quad (10)$$

which defines the natural inner product on the tangent space,

$$\langle \dot{q}_1, \dot{q}_2 \rangle_M := \dot{q}_1^T M \dot{q}_2, \quad (11)$$

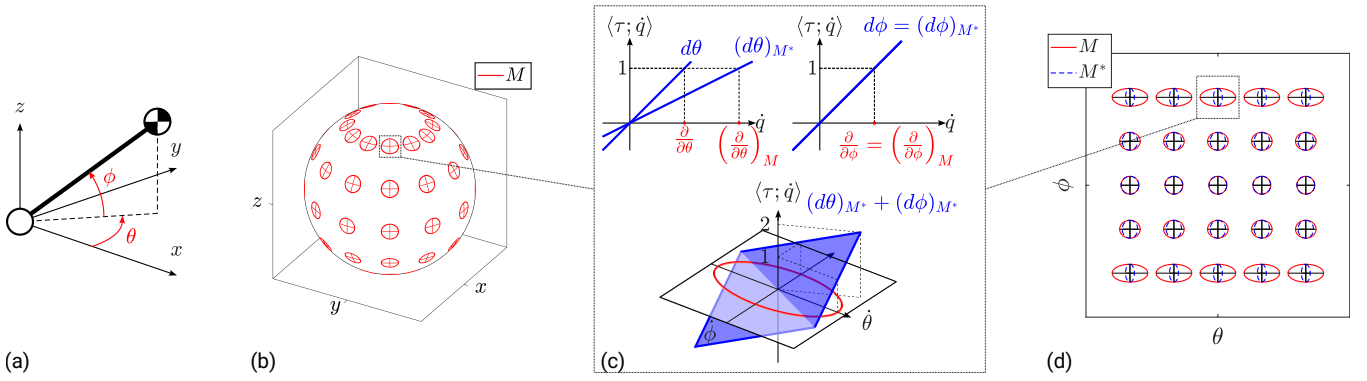


Fig. 2. Metric and dual-metric normalization illustrated by a pan-tilt mechanism. (a) A pan-tilt mechanism with a massless link and a point mass at the end effector; its generalized coordinates parameterize the configuration manifold through a nonlinear chart. (b) The Riemannian metric induced in the ambient Euclidean space by the point-mass motion constrained by the mechanism. The red ellipses denote the unit- M -norm set; their intercepts indicate the metric-normalized tangent directions at each configuration. (c) An M -orthonormal tangent basis and its dual co-basis, together with the vector-covector duality through power. The covector can be interpreted as a slope measuring how much power is produced by motion in a given direction. (d) The pullback of the metric and dual metric into coordinate space, visualized by the red and blue ellipses corresponding to unit velocity and force norms, respectively.

with associated norm

$$\|\dot{q}\|_M := \sqrt{\dot{q}^\top M \dot{q}}. \quad (12)$$

Geometrically, M measures generalized velocity after it has been mapped from coordinates into the ambient mechanical space, making coordinate velocities physically commensurate.

This interpretation is illustrated by the pan-tilt mechanism in Fig. 2(a). Let

$$q = \begin{bmatrix} \theta \\ \phi \end{bmatrix}, \quad (13)$$

where θ and ϕ denote pan and tilt. Let $x(q) \in \mathbb{R}^3$ denote the position of the point mass at the end effector. Its ambient velocity is

$$\dot{x} = J(q)\dot{q}, \quad (14)$$

where $J(q)$ is the Jacobian. If the ambient space is equipped with the Euclidean inner product, then the induced metric on generalized velocities is

$$M = J^\top(q)J(q), \quad (15)$$

and the physically meaningful squared speed is

$$\|\dot{x}\|_2^2 = \dot{q}^\top J^\top(q)J(q)\dot{q} = \dot{q}^\top M \dot{q}. \quad (16)$$

As shown in Fig. 2(b), the same coordinate increment can correspond to different ambient motions depending on configuration. This dependency is why a Euclidean norm on \dot{q} is not geometrically meaningful, whereas $\|\dot{q}\|_M$ measures the actual ambient motion.

For inertia-dominated systems, the natural metric is the inertia matrix, and the kinetic energy is

$$\text{KE}(q, \dot{q}) = \frac{1}{2} \dot{q}^\top M \dot{q}. \quad (17)$$

For drag-dominated systems, the natural metric is the drag matrix, and the drag dissipation power is

$$P(q, \dot{q}) = \dot{q}^\top M \dot{q}. \quad (18)$$

In both cases, M defines the physically meaningful norm of generalized velocity.

Let $\frac{\partial}{\partial q} = [\frac{\partial}{\partial q_1}, \dots, \frac{\partial}{\partial q_n}]$ denote the coordinate basis of $T_q Q$. One convenient choice of M -orthonormal tangent basis is

$$\left(\frac{\partial}{\partial q}\right)_M = \left(\frac{\partial}{\partial q}\right) M^{-\frac{1}{2}}, \quad (19)$$

so that

$$\left(\frac{\partial}{\partial q}\right)_M^\top M \left(\frac{\partial}{\partial q}\right)_M = \text{Id}. \quad (20)$$

Thus, the columns of $\left(\frac{\partial}{\partial q}\right)_M$ form tangent basis vectors with unit M -norm and mutual M -orthogonality. In Fig. 2(b), the unit- M -norm ellipse encodes these normalized tangent directions, and Fig. 2(c)–(d) illustrates the corresponding orthonormal tangent basis in coordinate and pulled-back form.

Generalized forces are covectors, i.e., elements of $T_q^* Q$, and pair with velocities to produce power:

$$P = \tau(\dot{q}) = \langle \tau; \dot{q} \rangle. \quad (21)$$

This vector-covector duality implies that force is naturally interpreted as the directional rate of power production per unit velocity.

Let $dq = [dq_1, \dots, dq_n]^\top$ denote the coordinate co-basis, which measures how the energy changes as each component of the configuration is incremented, as sketched in Fig. 2(c). The dual co-basis to $\left(\frac{\partial}{\partial q}\right)_M$ is

$$(dq)_{M^*} = M^{\frac{1}{2}} dq, \quad (22)$$

which satisfies

$$\left\langle (dq)_{M^*}^i; \left(\frac{\partial}{\partial q}\right)_M^j \right\rangle = \delta_{ij}. \quad (23)$$

Hence, each covector in the dual co-basis produces unit power when paired with the corresponding orthonormal

tangent basis vector and zero with the others. This is the dual structure illustrated in Fig. 2(c).

The metric on velocities induces the dual metric on the cotangent space. Since the dual co-basis is orthonormal, the induced dual metric is

$$M^* = M^{-1}, \quad (24)$$

with associated dual norm

$$\|\tau\|_{M^*} := \sqrt{\tau^\top M^* \tau}. \quad (25)$$

Thus, the dual metric is the natural metric for generalized forces: it is precisely the one compatible with M through vector–covector duality [21].

Returning to the pan–tilt example, let

$$\tau = \tau_\theta d\theta + \tau_\phi d\phi \quad (26)$$

denote the generalized torques. If torque residuals are measured using the Euclidean coordinate norm, then their relative importance depends on the chosen coordinate chart and scaling. Rescaling a coordinate changes the numerical representation of the torque covector, and the same coordinate norm can correspond to different physical power at different configurations, as suggested by Fig. 2(b) and Fig. 2(d). By contrast, the dual norm in (24) evaluates the covector using the geometry induced by the ambient mechanical space. In this way, the dual metric pulls the coordinate force back into the underlying physical space, just as M pulls the coordinate velocity back into that space.

Let

$$r_k(\pi) := Y_k \pi - \tau_k \quad (27)$$

denote the inverse-dynamics residual at sample k . Standard least squares minimizes the Euclidean coordinate norm $\|r_k(\pi)\|_2^2$, which depends on the coordinate chart. To measure force residuals in a coordinate-independent manner, we instead weight them by the dual metric:

$$\hat{\pi} = \arg \min_{\pi} \sum_{k=1}^N r_k(\pi)^\top M_k^*(\pi) r_k(\pi). \quad (28)$$

where M_k^* is the system dual metric evaluated at sample k . For inertia-dominated systems, M_k is the composite inertia matrix; for drag-dominated systems, M_k is the composite drag matrix. Equation (28) therefore defines a coordinate-independent identification objective: it measures force residuals through their physical power interpretation rather than through their raw coordinate representation.¹

¹Note that some system identification problems may not be fully observable [22]. Nevertheless, because the composite metric tensor typically appears directly in the inverse dynamics, dual-metric normalization preserves the same invariant set of dynamic parameters as the original regression. Therefore, the proposed method remains compatible with systems that are not fully identifiable, such as the Crazyflie–pendulum system studied here.

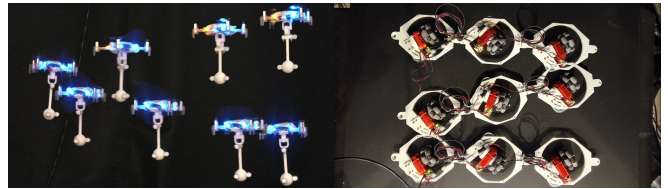


Fig. 3. Experimental platforms: the inertia-dominated Crazyflie with a pendulum attached through a universal joint (left), and the drag-dominated three-link LandSalp robot (right), together with snapshots of representative execution trajectories.

B. Convex Reformulation via Schur Complements

At first glance, (28) appears difficult to optimize because both the residual $r_k(\pi)$ and the weighting matrix $M_k^*(\pi)$ depend on the unknown parameters π . Nevertheless, the problem admits a convex reformulation.

For the system classes considered here, the metric is affine in the dynamic parameters:

$$M_k(\pi) = M_{k,0} + \sum_{i=1}^p \pi_i M_{k,i}, \quad (29)$$

where each $M_{k,i} \in \mathbb{S}^n$ is known for sample k , and $M_k \in \mathbb{S}_{++}^n$ is enforced through physical consistency constraints. Likewise,

$$r_k(\pi) = Y_k \pi - \tau_k \quad (30)$$

is affine in π . Thus, the only nonlinearity in (28) is the quadratic form involving the inverse of an affine matrix.

Introduce a slack variable $s_k \in \mathbb{R}$ for each sample and impose

$$s_k \geq r_k(\pi)^\top M_k^*(\pi) r_k(\pi). \quad (31)$$

By the Schur complement, (31) is equivalent to

$$\begin{bmatrix} M_k(\pi) & r_k(\pi) \\ r_k(\pi)^\top & s_k \end{bmatrix} \succeq 0, \quad (32)$$

provided that $M_k \succ 0$. Because both blocks are affine in π , (32) is a convex semidefinite constraint.

The original problem is therefore equivalent to

$$\hat{\pi} = \arg \min_{\pi, \{s_k\}} \sum_{k=1}^N s_k \quad \text{s.t. (32) } \forall k. \quad (33)$$

The objective is linear in the slack variables, and all constraints are convex. Hence, (33) remains a convex semidefinite program.

This reformulation shows that coordinate-independent system identification does not require giving up the computational advantages of inverse-dynamics least squares. Although the dual metric depends on the unknown parameters, its affine structure allows the weighted residual to be represented exactly through Schur-complement LMIs. The proposed method therefore preserves the practical tractability of convex identification while replacing the coordinate-dependent Euclidean force residual with a geometrically correct, coordinate-independent one.

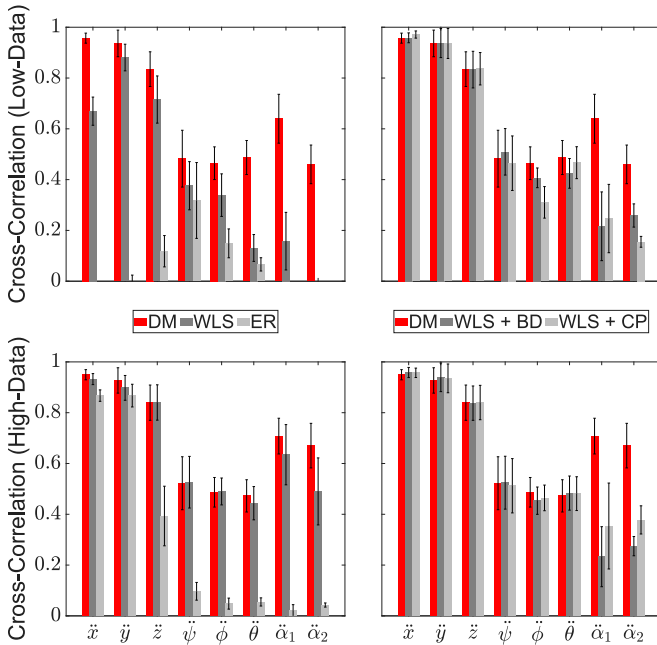


Fig. 4. Normalized cross-correlation between predicted and measured forward dynamics for the Crazyflie–pendulum system; larger values are better, and error bars indicate the standard deviation over the test set. The proposed method (DM) consistently outperforms the alternatives, especially on the shape coordinates ($\dot{\alpha}_1$ and $\dot{\alpha}_2$). Top: low-data case. Bottom: high-data case. Left: comparison with WLS and energy-based least squares. Right: comparison with regularized WLS using Bregman divergence and constant pullback.

IV. EXPERIMENTS

We evaluated the proposed method on two robotic systems with qualitatively different dynamics: a Crazyflie 2.0 quadrotor with a pendulum attached through a universal joint, and the LandSalp robot (Fig. 3). These systems are, respectively, inertia-dominated and viscous drag-dominated, matching the two classes of dynamics studied in this paper. They also provide challenging testbeds for coordinate-dependent identification: their generalized coordinates have different units and scales, admit multiple reasonable coordinate choices, and induce configuration-dependent inner products under the corresponding system metrics. For floating-base coordinates, we use body velocity and body-velocity change rate as \dot{q} and \ddot{q} , respectively.

For both platforms, we recorded data using an OptiTrack motion capture system together with onboard sensing. We compared the proposed dual-metric-WLS against error-covariance-WLS, energy-based least squares, and two regularized WLS variants using Bregman-divergence and constant-pullback regularizers. For the regularized methods, the error covariance is first estimated from the corresponding unregularized problem, following [18]. All methods were required to satisfy the same physical-consistency constraints.

We evaluated all methods in two cases: a practical low-data case, constructed by downsampling the processed training

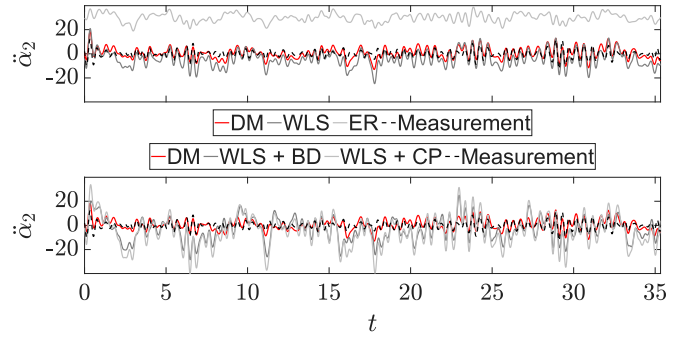


Fig. 5. Predicted and measured $\ddot{\alpha}_2$ for the Crazyflie–pendulum system in the high-data case, comparing the proposed method, WLS, energy-based least squares, and the two regularized WLS variants.

data,² and an ideal high-data case, using the full training set so that the assumptions behind error-covariance weighting are better satisfied. As the primary metric, we report the normalized cross-correlation between predicted and measured forward-dynamics signals at each coordinate. For each coordinate, we report the maximum normalized cross-correlation over time shifts within $\pm 5^\circ$ of the slowest motion period. This metric is more appropriate than trajectory RMSE because RMSE depends on the coordinate representation and is highly sensitive to small phase shifts. For coordinates with the largest performance differences, we also plot representative predicted and measured trajectories.

A. Inertia-Dominated System

The inertia-dominated platform is a Crazyflie 2.0 with a pendulum attached through a universal joint. Based on prior work [23], the system is differentially flat, with flat outputs given by the quadrotor x -, y -, and z -positions and yaw. We generated excitation trajectories using sinusoidal motions with mutually non-harmonic frequencies so that the full trajectory did not repeat over the experiment duration.

In addition to motion-capture measurements, we recorded onboard IMU data, battery voltage, and PWM commands to the four thrusters, all at 100 Hz. Generalized forces were computed from PWM and battery voltage using firmware calibration values. We collected six trajectories for training and six for testing; each lasted about 35 s, and each test trajectory started from a different phase. The identified parameters include the mass, center-of-mass moments, and inertia tensors of the quadrotor body, universal-joint core, and pendulum. Nominal values for the regularized baselines were obtained from the CAD model and UAV datasheet.

In the low-data case, we downsampled the processed training set to about 20 samples. As shown in the top panel of Fig. 4, the proposed method significantly outperformed WLS and the energy-based method, with the largest gains in body angular accelerations and pendulum shape accelerations. Compared with the regularized baselines, it achieved similar

²Downsampling is applied after preprocessing and regressor construction, and the downsampled identification regression remains the same rank as the full-data regression for both the inertia- and drag-dominated systems.

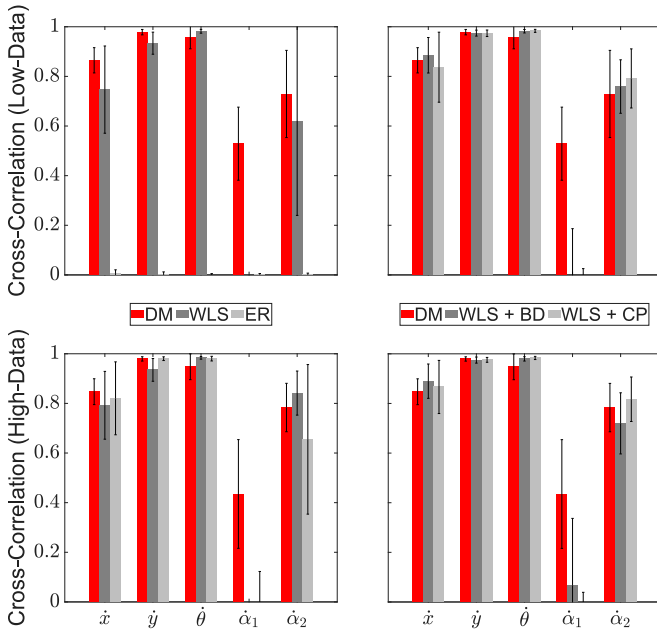


Fig. 6. Normalized cross-correlation between predicted and measured forward dynamics for the LandSalp system; larger values are better, and error bars indicate the standard deviation over the test set. The proposed method (DM) consistently outperforms the alternatives, especially on the shape coordinates ($\dot{\alpha}_1$ and $\dot{\alpha}_2$). Top: low-data case. Bottom: high-data case. Left: comparison with WLS and energy-based least squares. Right: comparison with regularized WLS using Bregman divergence and constant pullback.

performance on body linear and angular coordinates while still outperforming them on the pendulum shape coordinates.

Using the full training set, most methods performed similarly on body translation and attitude, but the proposed method still outperformed all alternatives on the two pendulum shape coordinates (bottom panel of Fig. 4). Thus, even when covariance weighting is well supported statistically, coordinate-independent weighting remains beneficial for internal shape dynamics.

Figure 5 shows a representative pendulum pitch-shape-acceleration trajectory. The proposed method captures most of the motion, whereas WLS and the energy-based method produce incorrect predictions. This result reflects the central geometric issue: residuals measured directly in the gimbal coordinates are distorted by the nonlinear coordinate representation, while the dual metric pulls them back into the ambient mechanical space.

B. Drag-Dominated System

The drag-dominated platform is the LandSalp robot, a multibody locomotion system with three omni wheels driven by series elastic actuators and two passive joints. The training trajectory consisted of eight excitation segments totaling about three minutes, generated by driving the three wheels through distinct sinusoidal combinations. Test trajectories consisted of forward, backward, leftward, rightward, and turning gaits from prior work [17]. In addition to motion-capture data, we recorded actuator force measurements.

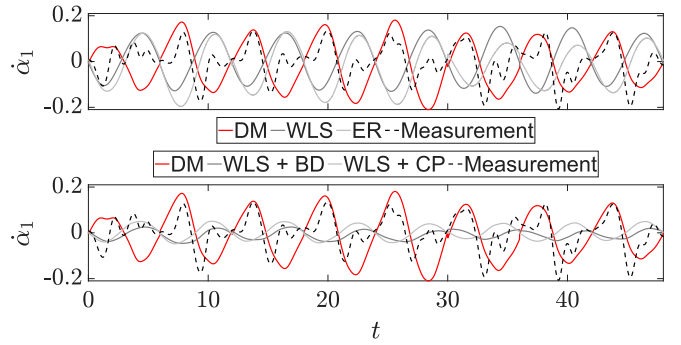


Fig. 7. Predicted and measured $\dot{\alpha}_1$ for the LandSalp system in the high-data case, comparing the proposed method, WLS, energy-based least squares, and the two regularized WLS variants.

The identified parameters include viscous drag coefficients for each body unit and joint, as well as the internal drag coefficient of each actuator. Identification was performed in two stages: actuator identification from output force, actual velocity, and commanded velocity; then link and joint drag identification using the inverse-dynamics framework in this paper. Nominal values for the regularized baselines were taken from prior identification results [17].

In the low-data case, we downsampled the processed training set to about 40 samples. As shown in the top panel of Fig. 6, the proposed method outperformed WLS, the energy-based method, and the regularized baselines on the shape coordinates. The largest contrast appeared in the first shape coordinate, where all competing methods except the proposed one exhibited non-positive cross-correlation, indicating predictions roughly 90° to 180° out of phase with the measurements.

Using the full training set, the qualitative result remained the same (bottom panel of Fig. 6). Although the competing methods performed similarly on body position and orientation, the proposed method still outperformed all alternatives on the shape coordinates.

Figure 7 shows a representative first-joint-velocity trajectory during leftward motion. The proposed method captures most of the joint motion, whereas WLS and the energy-based method show large phase errors. As in the Crazyflie experiment, this result indicates that residuals measured directly in joint coordinates are distorted by the nonlinear coordinate representation, while dual-metric weighting recovers the underlying physical information more faithfully.

C. Discussion

Across both robotic systems, the proposed method performed consistently in both low-data and high-data cases. This robustness suggests that its advantage is geometric rather than merely statistical: by pulling residuals back into the ambient mechanical space, the dual metric removes coordinate dependence and improves data efficiency.

By contrast, the energy-based method consistently performed poorly, likely because its effectively rank-one weighting compresses vector residual information into a single

scalar channel, reducing identifiability and worsening conditioning. WLS improved only when enough data were available to estimate the residual covariance reliably, yet it remained less effective on shape coordinates, where nonlinear coordinate representations are most severe. The regularized baselines benefited from additional prior information, but they still inherited the coordinate dependence of the underlying residual and may be less reliable in practice when nominal parameters are unavailable or inaccurate.

In addition to improved accuracy, the proposed method was also numerically more robust in practice. The dual metric acts as a physically meaningful self-scaling mechanism, substantially reducing the need for manual scaling and numerical tuning compared with the competing methods.

V. CONCLUSION AND FUTURE WORK

This paper proposed a coordinate-independent system identification method by applying dual metrics as weights in inverse-dynamics least squares. By using the dual metric induced by the system Riemannian metric, the method measures residuals in a physically meaningful way, pulling coordinate force residuals back into the ambient mechanical space and eliminating dependence on coordinate choice, units, and scaling. The resulting objective remains a convex optimization problem through an affine-metric and Schur-complement reformulation, while remaining compatible with physical-consistency constraints and geometric regularization. Experiments on an inertia-dominated Crazyflie–pendulum system and a drag-dominated LandSalp robot showed the best average performance across both low-data and high-data settings, with the largest gains on shape coordinates, where nonlinear coordinate representations make coordinate dependence most severe. These results show that coordinate independence is not only a geometric property, but also a practical source of robustness and data efficiency in robot model identification.

Future work includes extending this coordinate-independent viewpoint to broader identification settings in which time-domain data on manifolds is used, such as likelihood-based neural ODE or neural SDE models [15]. Another direction is online parameter estimation, where the dual-metric weighting may need efficient updates or approximations during adaptation. It is also important to study systems governed by multiple metrics, especially when different physical effects dominate on different time scales. Finally, incorporating sample independence into the objective may improve robustness to repeated or redundant data and clarify its relationship to identifiability.

REFERENCES

- [1] R. Featherstone and D. Orin, “Robot dynamics: Equations and algorithms,” in *Proceedings 2000 ICRA. Millennium Conference. IEEE International Conference on Robotics and Automation. Symposia Proceedings (Cat. No.00CH37065)*, vol. 1. San Francisco, CA, USA: IEEE, 2000, pp. 826–834.
- [2] E. Todorov, T. Erez, and Y. Tassa, “MuJoCo: A physics engine for model-based control,” in *2012 IEEE/RSJ International Conference on Intelligent Robots and Systems*. Vilamoura-Algarve, Portugal: IEEE, Oct. 2012, pp. 5026–5033.
- [3] T. D. Barfoot, *State Estimation for Robotics*, 1st ed. Cambridge University Press, July 2017.
- [4] P. M. Wensing, M. Posa, Y. Hu, A. Escande, N. Mansard, and A. D. Prete, “Optimization-Based Control for Dynamic Legged Robots,” *IEEE Transactions on Robotics*, vol. 40, pp. 43–63, 2024.
- [5] S. Rezazadeh, A. Abate, R. L. Hatton, and J. W. Hurst, “Robot Leg Design: A Constructive Framework,” *IEEE Access*, vol. 6, pp. 54 369–54 387, 2018.
- [6] A. Kadian, J. Truong, A. Gokaslan, A. Clegg, E. Wijmans, S. Lee, M. Savva, S. Chernova, and D. Batra, “Sim2Real Predictivity: Does Evaluation in Simulation Predict Real-World Performance?” *IEEE Robotics and Automation Letters*, vol. 5, no. 4, pp. 6670–6677, Oct. 2020.
- [7] E. Aljalbout, J. Xing, A. Romero, I. Akinola, C. R. Garrett, E. Heiden, A. Gupta, T. Hermans, Y. Narang, D. Fox, D. Scaramuzza, and F. Ramos, “The Reality Gap in Robotics: Challenges, Solutions, and Best Practices,” *Annual Review of Control, Robotics, and Autonomous Systems*, Dec. 2025.
- [8] T. Lee, J. Kwon, P. M. Wensing, and F. C. Park, “Robot Model Identification and Learning: A Modern Perspective,” *Annual Review of Control, Robotics, and Autonomous Systems*, vol. 7, no. 1, pp. 311–334, July 2024.
- [9] R. Pintelon and J. Schoukens, *System Identification: A Frequency Domain Approach*, 2nd ed. Piscataway, NJ: IEEE Press, 2012.
- [10] C. G. Atkeson, C. H. An, and J. M. Hollerbach, “Estimation of Inertial Parameters of Manipulator Loads and Links,” *The International Journal of Robotics Research*, vol. 5, no. 3, pp. 101–119, Sept. 1986.
- [11] A. Zeng, S. Song, J. Lee, A. Rodriguez, and T. Funkhouser, “TossingBot: Learning to Throw Arbitrary Objects With Residual Physics,” *IEEE Transactions on Robotics*, vol. 36, no. 4, pp. 1307–1319, Aug. 2020.
- [12] B. Bittner, R. L. Hatton, and S. Revzen, “Data-driven geometric system identification for shape-underactuated dissipative systems,” *Bioinspiration & Biomimetics*, vol. 17, no. 2, p. 026004, Mar. 2022.
- [13] S. L. Brunton and J. N. Kutz, *Data-Driven Science and Engineering: Machine Learning, Dynamical Systems, and Control*, 1st ed. Cambridge University Press, Jan. 2019.
- [14] L. Manuelli, Y. Li, P. Florence, and R. Tedrake, “Keypoints into the future: Self-supervised correspondence in model-based reinforcement learning,” in *Proceedings of the 2020 Conference on Robot Learning*, ser. Proceedings of Machine Learning Research, J. Kober, F. Ramos, and C. Tomlin, Eds., vol. 155. PMLR, Nov. 2021, pp. 693–710.
- [15] R. T. Q. Chen, Y. Rubanova, J. Bettencourt, and D. K. Duvenaud, “Neural ordinary differential equations,” in *Advances in Neural Information Processing Systems*, S. Bengio, H. Wallach, H. Larochelle, K. Grauman, N. Cesa-Bianchi, and R. Garnett, Eds., vol. 31. Curran Associates, Inc., 2018.
- [16] S. Greydanus, M. Dzamba, and J. Yosinski, “Hamiltonian neural networks,” in *Advances in Neural Information Processing Systems*, H. Wallach, H. Larochelle, A. Beygelzimer, F. dAlché-Buc, E. Fox, and R. Garnett, Eds., vol. 32. Curran Associates, Inc., 2019.
- [17] Y. Yang, N. L. Hecht, Y. Salaman-Maclara, N. Justus, Z. A. Thomas, F. Rozaidi, and R. L. Hatton, “Geometric data-driven multi-jet locomotion inspired by salps,” *arXiv:2503.08817 [cs.RO]*, 2025.
- [18] T. Lee, P. M. Wensing, and F. C. Park, “Geometric Robot Dynamic Identification: A Convex Programming Approach,” *IEEE Transactions on Robotics*, vol. 36, no. 2, pp. 348–365, Apr. 2020.
- [19] P. M. Wensing, S. Kim, and J.-J. E. Slotine, “Linear Matrix Inequalities for Physically Consistent Inertial Parameter Identification: A Statistical Perspective on the Mass Distribution,” *IEEE Robotics and Automation Letters*, vol. 3, no. 1, pp. 60–67, Jan. 2018.
- [20] M. Gautier, “Dynamic identification of robots with power model,” in *Proceedings of International Conference on Robotics and Automation*, vol. 3. Albuquerque, NM, USA: IEEE, 1997, pp. 1922–1927.
- [21] A. Cabrera and R. L. Hatton, “Optimal control of robotic systems and biased Riemannian splines,” *ESAIM: Control, Optimisation and Calculus of Variations*, vol. 30, p. 36, 2024.
- [22] P. M. Wensing, G. Niemeyer, and J.-J. E. Slotine, “A geometric characterization of observability in inertial parameter identification,” *The International Journal of Robotics Research*, vol. 43, no. 14, pp. 2274–2302, Dec. 2024.
- [23] K. Sreenath, Taeyoung Lee, and V. Kumar, “Geometric control and differential flatness of a quadrotor UAV with a cable-suspended load,” in *52nd IEEE Conference on Decision and Control*. Firenze: IEEE, Dec. 2013, pp. 2269–2274.